Journal of the Indian Society of Remote Sensing (May 2021) 49(5):1121–1139
https://doi.org/10.1007/s12524-020-01295-1

RESEARCH ARTICLE

Coupling Remote Sensing and GIS with KINEROS2 Model for Spatially Distributed Runoff Modeling in a Himalayan Watershed

Sameer Saran[1] · Geert Sterk[2] · S. P. Aggarwal[1] · V. K. Dadhwal[3]

Received: 30 July 2020 / Accepted: 15 December 2020 / Published online: 19 January 2021

Abstract

Excessive runoff and high soil erosion rate are the critical problems in the Himalayan terrain, mainly due to rugged topography and high intensity rains. Accurate quantification of runoff and erosion is thus of paramount importance for taking appropriate measures to sustain the soil productivity in the Himalayan watersheds. Distributed, process-based hydrological and erosion models are ideal for this purpose. However, model parameterization in the rugged, inaccessible and thus generally a data scarce Himalayan watershed is a major challenge. The present study primarily investigates the applicability of kinematic runoff and erosion model (KINEROS2) model in a Himalayan watershed besides exploring the potential of satellite remote sensing and GIS in spatially distributed runoff modeling. The KINEROS2 model, is an event-based, distributed, water and erosion process model. It discretizes the watershed into a mosaic of planes and channels based on topography. The runoff is estimated for each plane which eventually flows to adjacent channel and is then routed to estimate the total runoff at the watershed outlet. Remote sensing is primarily used for model parameterization, i.e., characterizing the individual planes and channels. Optimized digital elevation model and fine-scale land-use/land-cover information are generated using high-resolution panchromatic and multi-spectral optical and microwave satellite imagery. The resulting data on near-surface soil moisture from radar imagery (ENVISAT ASAR) calibrated the initial soil moisture in the model, whose performance is evaluated using root mean square error and Nash–Sutcliffe that reveals that KINEROS2 model works quite well in a small Himalayan watershed. The sensitivity analysis indicates that saturated soil hydraulic conductivity is the most sensitive parameter influencing the runoff compared to Manning's coefficient and initial soil moisture. The model output is also used for validating the remote sensing and geographical information system (GIS) based hydrologic response units delineated in a previous research study. The study highlights that the coupling of remote sensing and GIS with process models, such as KINEROS2, can provide valuable information in planning sustainable watershed management practices in the Himalayan watersheds.

Keywords Remote sensing · KINEROS2 model · Hydrological modeling · Hydrologic response units · Himalaya

✉ Sameer Saran
sameer@iirs.gov.in

Geert Sterk
G.Sterk@uu.nl

S. P. Aggarwal
spa@iirs.gov.in

V. K. Dadhwal
vkdadhwal@iist.ac.in

[1] Indian Institute of Remote Sensing, Indian Space Research Organisation, #4, Kalidas Road, Dehradun 248001, India

[2] Utrecht University, Utrecht, The Netherlands

[3] Indian Institute of Space Science and Technology, Trivandrum, India

Introduction

The Himalaya is known as one of the most fragile ecosystems region on the earth (Tiwari 2000) and poses a serious threat to sustenance of soil productivity due to excessive runoff and high erosion which leads to the land degradation process. The primary causes of erosion include deforestation, terrain steepness, high intensity rain leading to excessive runoff generation, overgrazing, tectonics, intensive and subsistence farming. The Sub-Himalayan hill ranges, lying in the foothills of the main Himalayan belt, are particularly susceptible to high rate of soil erosion and sedimentation owing to steep slopes, depleted forest cover

due to high population pressure, and young geologic materials (Jain et al. 2001). As mentioned by Morgan (2001), the soil erosion is directly linked with the long-term consequences of sustainable agriculture and soil productivity, hence, finding the spatial distribution of those areas which are prone to land degradation and assessment of the erosion risk severity are of paramount importance.

Many hydrological models are utilized to quantify the runoff and sediment yield for planning conservation strategies in the watersheds. These models range from fully empirical to fully deterministic and from lumped to spatially distributed models; many intermediate types exist as well (Morgan 2005). The distributed, deterministic models attempt to describe the physical processes associated with runoff and water erosion at all locations in the spatial modeling domain and at every time-step. Process description includes rainfall interception by canopy, infiltration, sub-surface flow, overland flow, splash detachment by raindrops, sediment transport and deposition (Beven 2012). For detailed assessments of runoff like for instance at watershed level, application of a spatially explicit, deterministic model is potentially useful. It enables delineating areas with higher runoff and erosion risks within the watershed and understanding the underlying factors at different spatial locations. The drawback of these models is the large input data requirement at every spatial unit the watershed is discretized into. Obtaining the effective values of all the variables that describes the physical methods at each spatial unit limit the applicability of distributed, deterministic models (Beven 2012). By implementing the remote sensing and geographical information systems (GIS), the spatially distributed model of various processes of watershed hydrology is developed for incorporating the spatial forms of soils, terrain and vegetation. However, the results of various studies uncovered the consequences of hydrological simulations are considerably inclined by the land-use/land-cover (LULC), soil properties and topographical data quality (Kite 1995; Wolock and Price 1994). The watershed is divided by the hydrological models into the *hydrological response units* (HRUs) with similar hydrological behavior as a spatial unit. The fundamental principles of characterizing the similarity of each HRUs are dependent on the hydrological systems analysis, in which, variety of hydrological dynamics inside individual HRUs are little contrasted with the alteration of neighboring HRUs (Flügel 1997). These models are united by GIS to provide and analyze unlike LULC maps and pedo-topo-geological links. These independently stored spatial records provide data which is surely appropriate to hydrological modeling instead of providing information on its direct usage (Beven 2012). In GIS, the overlay analysis of independent layers may assist to categorize similar landscape elements into the hydrological lumped units for the rainfall-runoff modeling.

Accurate parameterization of hydrological models is an essential step as slight errors in input parameters may lead to uncertainty in model outputs. GIS and satellite remote sensing techniques have proven as a vital source of spatially distributed data for hydrological modeling (Band and Moore 1995; Famiglietti and Wood 1994; King and Delpont 1993; Moore et al. 1991, 1993; Quincey et al. 2007; Siakeu and Oguchi 2000; Star et al. 1997; Vrieling 2006; Wigmosta et al. 1994). Some of the land surface parameters estimated from the remote sensing imagery are extremely useful in characterizing the watershed attributes. The optical remote sensing datasets are operationally used to map and monitor different LULC types and their biophysical characterization. Some of the limitations of optical remote sensing are overcome nowadays by microwave remote sensing, which is appropriate for assessing the soil's hydrological state mainly because of the all-weather capability and the sensor's sensitivity to the dielectric surface properties, depending on soil moisture content (van Oevelen 1994). The sensitivity of microwaves to surface roughness is especially useful in characterizing the hydrological and erosion processes through hydrological models (Baghdadi et al. 2002). However, significant advancements have been made in assessing the profile and near-surface content of soil water and hydraulic properties using model inversion, for example, Entekhabi et al. (1994). Further, microwave data being sensitive to vegetation structure can be fused with optical data to better characterize the vegetation parameters and LULC.

Hydrological modeling in the Himalayan watersheds is often a challenge due to difficulty in accurate and effective model parameterization. The data available in such mountainous watersheds are generally point measurements and are limited in number due to inaccessibility and time constraints. Since hydrological models require input parameter values at all the spatial modeling units, upscaling of limited point measurements to the spatial hydrologic units is a major issue. Satellite remote sensing by virtue of providing the synoptic view is the only practically viable option for upscaling the point measurements in such data-scarce watersheds. Thus, remote sensing is helpful in parameterization of distributed hydrological models by providing accurate information about the spatial variability of different watershed attributes even in data- scarce region.

In order to investigate the applicability of remote sensing and GIS techniques in characterizing the hydrological processes in the Himalayan watersheds, a research study is initiated recently. Sitla Rao watershed in the Sub-Himalaya near Dehradun (India) is taken as the study site. Various digital image processing, photogrammetric and GIS-based

techniques are used to obtain information on different watershed characteristics relevant to understanding the hydrological processes. These include: (i) LULC characterization using remote sensing data—microwave and optical (Saran et al. 2009); (ii) soil moisture estimation of near-surface in a spatially distributed manner from microwave remote sensing using ENVISAT ASAR data (Saran et al. 2014); and (iii) preparation of optimal *digital elevation model* (DEM) based on comparative evaluation of different remote sensing-derived DEMs and delineation of HRUs using topography (DEM), LULC and soil depth for qualitative characterization of runoff potential across the watershed (Saran et al. 2010).

As an extension of this work, the present study primarily investigates the applicability of KINEROS2 model in the Himalayan watershed besides exploring the potential of satellite remote sensing and GIS in spatially distributed runoff modeling. The KINEROS2 model (Smith et al. 1995) is an event-based, distributed, process model that simulates runoff and soil erosion in small watersheds by discretizing them into small planes and channels based on topography, and further allows integration of LULC, soil, and field datasets. The specific objectives of the study are to: (i) model event-based runoff using KINEROS2 model by combining remote sensing and field data; (ii) calibrate and validate the model based on rainfall events of different intensities; (iii) perform sensitivity analysis for identifying the significant parameter(s) influencing the rainfall-runoff processes; and (iv) to validate the previously delineated remote sensing and GIS-based HRUs with the KINEROS2 model results.

A Kinematic Runoff and Erosion Model (KINEROS2 Model)

Model Description

KINEROS2 model is a physical, distributed, process-based and event-based model developed to explain the procedures of erosion and runoff from lesser agricultural watersheds (Smith et al. 1995; Woolhiser et al. 1990). It segregates the model domain into a joint set of planes and channels based on topography. The channels allow the water and sediments that flows over multiple hierarchical planes. The LULC, soil and field datasets are integrated to incorporate the infiltration, rainfall, erosion and runoff parameters along with individual planes and channels into the model. It also uses small detention reservoirs, urban developments, sediment yield and lined channels on flood hydrograph. The parameter characteristics of planes and channels are shown in Tables 1 and 2.

The overland condition occurs if the rainfall intensity exceeded the soil's infiltration capacity. KINEROS2 uses a generalized Smith-Parlange model to estimate infiltration (Parlange et al. 1982) by incorporating the models of Smith and Parlange (1978) and Green and Ampt (1911) as restricting circumstances. The infiltration capacity, $f_c(t)$, is estimated as:

$$fc(t) = K_s \left\{ 1 + \omega / e^{\omega F(t)/[(G+h)(\Phi-\theta_i)]-1} \right\} \quad (1)$$

where $F(t)$ represents cumulative infiltration depth of water in soil, h is the flow depth, Φ refers soil absorbency, θ_i is the initial soil moisture content prior to the event, ω is a parameter between zero and one, K_s is the soil hydraulic conductivity, and G is the net capillary drive parameter.

KINEROS2 uses a kinematic wave approximation to simulate flow over individual rectangular planes, and solves the continuity equation as:

$$\frac{\partial h}{\partial t} + \alpha m h^{m-1} \frac{\partial h}{\partial x} = q_L(x,t) \quad (2)$$

where t is time, x is the distance along the slope direction, α and m parameters are related to slope, q_L refers to lateral inflow rate, flow regime and surface roughness. The relationship between unit flow discharge, q and flow depth, h is shown as follows:

$$q = \alpha h^m \quad (3)$$

The overland flow entering the channel is then routed to the watershed outlet.

Customized Geospatial Tool: Automated Geospatial Watershed Assessment Tool (AGWA)

The AGWA is a GIS-enabled tool that runs KINEROS2 model in a spatial domain. It was developed in 2002 by the USDA-ARS, US Environmental Protection Agency (EPA) Office of Research and Development (ORD), and the University of Arizona (UA) (Miller et al. 2002). It is openly available on the web as a suite of modular and open-source programs (www.tucson.ars.ag.gov/agwa or www.epa.gov/nerlesdl/land-sci/agwa). The tool facilitates watershed discretization, parameterization, calibration, simulation and validation of the model (Miller et al. 2007). The AGWA tool helps to subdivide the watershed into model elements (planes and channels) using topography (first-order derivate of DEM) and these model elements are further spatially joined with soil and land use based hydrological properties as defined in Tables 1 and 2. In addition, the AGWA facilitates the conception and comparison of results in spatial domain and therefore, allows for evaluation of hydrologic behavior within a selected landscape (Semmens et al. 2008).

Table 1 Planes parameter characteristics (Woolhiser et al. 1990)

SI. no.	Plane parameters	Definition of parameters
1	Length	Length (m)
2	Width	Width (m)
3	Slope	Slope (rise/run)
4	Manning	Roughness coefficient ($sm^{-1/3}$)
5	K_s	Saturated hydraulic conductivity (mm/hr)
6	G	Mean capillary drive, mm – a zero value sets the infiltration at a constant value of K_s
7	Porosity	Porosity
8	ROCK	Volumetric rock fraction
9	DIST	Pore size distribution index. This parameter is used for redistribution of soil moisture during unponded intervals
10	CV	Coefficient of variation of K_s
11	INTER	Interception depth (mm)
12	CANOPY	Cover fraction of surface covered by intercepting cover-rainfall intensity is reduced by this fraction until the specified interception depth has accumulated
13	FRACT	List of particle class fraction
14	SPLASH	Rain splash coefficient
15	COH	Soil cohesion coefficient

Table 2 Channel parameter characteristics (Woolhiser et al. 1990)

S. no.	Channel parameters	Definition of parameters
1	Upstream	Upstream Identifier(s) to ten upstream contributing elements
2	Lateral	Identifier(s) of up to two plane elements contributing lateral inflow
3	Length	Length (m)
4	Width	Bottom Width (m)
5	Slope	Bottom Slope (rise/run)
6	Manning	Roughness coefficient ($sm^{-1/3}$)
7	SAT	Initial degree of soil saturation, expressed as a fraction of pore space filled
8	SS1, SS2	Bank side slopes—right or left
9	K_s	Saturated hydraulic conductivity (mm/hr)
10	G	Mean capillary drive, mm—a zero value sets the infiltration at a constant value of K_s
11	Porosity	Porosity
12	ROCK	Volumetric rock fraction
13	DIST	Pore size distribution index. This parameter is used for redistribution of soil moisture during unponded intervals
14	COH	Soil cohesion coefficient
15	FRACT	List of particle class fractions
16	TYPE	Simple or Compound

Previous Work

The earlier and the most recent development of KINEROS model has been comprehensively elaborated and nicely discussed by Goodrich et al. (2012). The model was initially conceptualized and described during 1960s primarily focusing toward routing surface runoff over course of overland flow planes and afterward merging to channels (Woolhiser et al. 1970). An interactive infiltration component was added to the model subsequently (Rovey et al. 1977). The model was further enhanced by incorporating erosion and sediment transport component (Woolhiser et al. 1970; Smith et al. 1995). Subsequently there were slight modifications incorporated in the model like

modification of the infiltration component, addition of pond elements, modification of the input to allow spatial variability of rainfall, and accounting for small-scale spatial variation of saturated hydraulic conductivity. After all modifications and enhancements, the open-source based robust KINEROS2 is known as K2 model which is freely available through the KINEROS2 website. This K2 model was documented, released and applied to various application domains (Woolhiser et al. 1990; Smith et al. 1995; Woolhiser et al. 1996; Goodrich et al. 2004; Goodrich et al. 2012). The KINEROS model was implemented, calibrated and validated at various spatio-temporal scales on different storm events over variety of watersheds situated across the world. Table 3 summarizes KINEROS model based research studies with specific aims and objectives.

Materials and Methods

Study Area

The area selected for this experimental study is a part (sub-watershed) of Sitla Rao watershed, located in western part of Dehradun in the Sub-Himalaya of North India (Fig. 1). Its geographic aspect of the watershed reaches out from 30° 24′ 39“ to 30° 29′ 05” N latitudes and 77° 45′ 33“ to 77° 57′ 46” E longitudes, while the sub-watershed extends from 30° 28′ 17.56“ to 30° 28′ 39.45” N latitudes and 77° 54′ 39.17“ to 77° 55′ 26.61” E longitudes. The area of the Sitla Rao watershed is at 400–2200 m above of mean sea level with 5800 ha, while size and altitude of the sub-watershed is 41.6 ha and 885 to 1202 m, respectively. The geomorphology of this study region establishes a series of slopes in the upper part with river valleys, and watershed with wide piedmonts in center and bottom part. The gradient in the watershed differs from moderate (< 15%) in lower part to steep (> 45%) in the upper part, and generally, the soils vary from loam to sandy loam based on the different textures characteristics. Based on the similarities in slope, relief, geology, and landform features, the area is categorized into the following four major components—hillside slope, upper, middle and lower piedmont.

The annual rainfall is completely dependent on the elevation and varies from ∼ 1600 mm in the lower part to 2200 mm in the upper part of the watershed. Most of the rainfall occurs during the monsoon season, *i.e.,* mid-June to September and during summer, the mean monthly temperature ranges from ∼ 15 °C in winter to ∼ 33 °C. The main cropping seasons are Kharif (summer crop, June-September) and Rabi (winter crop, December-March). Mostly paddy rice and maize are grown in the Kharif season, whereas wheat is cultivated during the Rabi season. However, the key issue of farmers is of soil erosion, mainly in the steeper slopes, and to reduce its risk, the farmers practices for the terrace farming for the paddy rice. In addition, some other few measures for water and soil preservation are utilized for other yield types as well. The foremost LULC in the watershed is agriculture, settlements, forest and scrub. However, majority of the study area is occupied by the forest, especially, *Shorea robusta* (sal trees), which is categorized into different densities classes such as degraded (< 10%), open (10–40%) and dense (> 40%). The modeling site (sub-watershed) is dominated by agricultural land-use.

Field Data Collection

KINEROS2 model requires information on climate, terrain and soil characteristics to simulate runoff and sediment loss in the watershed. Soil texture map prepared earlier by the Agriculture and Soils Department of Indian Institute Remote Sensing, Dehradun, has been taken as the basic input to the model to derive saturated hydraulic conductivity (K_s), coefficient of variation of K_s, soil porosity, pore distribution index, mean capillary drive etc. parameters used in the KINEROS2 model. Field measurements on rainfall, runoff, soil moisture (infiltration and near-surface soil moisture) and surface roughness measurements were made during the monsoon period as described below.

Rainfall and Runoff Measurements

Rainfall was recorded using a self-recording rain gauge and runoff measurement was made using a flume, installed at the outlet of the sub-watershed (experimental site). Seven rainfall events of different intensities, for which corresponding runoffs were recorded, have been used in the present study (Table 4). Of the seven rainfall events (E1 to E7), four events (E1, E2, E3 and E5) are used for calibrating the model, while the remaining three rainfall events (E4, E6 and E7) are used for validating the model. The rainfall events for model calibration and validation are chosen in such a way that they represent different rain intensities.

Soil Moisture and Surface Roughness

Field data on soil moisture and surface roughness were collected in 21 agricultural fields concurrently with satellite data acquisition and the sampling was completed within 2 h of the satellite (ENVISAT ASAR) overpasses (Table 5). The ENVISAT ASAR products have geometric resolution of ∼ 30 m. The sampling sites were chosen using soil and crop type, elevation, slope, LULC classes and accessibility (Saran et al. 2014), and the fields were in

Table 3 Review of KINEROS model based research studies

Title of study	References	Objectives of the study
Investigating prediction capability of HEC-1 and KINEROS kinematic wave runoff models	Duru and Hjelmfelt (1994)	Comparison of HEC-1 and KINEROS models
Effects of rainfall sampling errors on simulation of desert flash floods	Michaud and Sorooshian (1994)	Flash flood forecasting with certain data constraints
Simulation of selected events on the Catsop catchment by KINEROS2: A report for the GCTE conference on catchment scale erosion models	Smith et al. (1999)	To simulate the runoff and sediment production (certain aspects of erosion simulation and the difficulties presented by unknown variables were highlighted)
Dynamics and scale in simulating erosion by water	Smith and Quinton (2000)	To assess the necessary spatial complexity to model runoff and erosion, considering scale
Erosion prediction on unpaved mountain roads in northern Thailand: validation of dynamic erodibility modeling using KINEROS2	Ziegler et al. (2001)	Predicting road runoff and erosion on an unpaved road in Pang Khum Experimental watershed (PKEW) in northern Thailand
Effect of geomorphologic resolution on modeling of runoff hydrograph and sedimentograph over small watersheds	Kalin et al. (2003)	Developing a quantitative relationship between peak runoff, basin characteristics and nature of storm for single events and also to analyze the effect of geomorphologic resolution on runoff hydrographs and sedimentographs over two small watersheds
Comparative assessment of two distributed watershed models with application to a small watershed	Kalin and Hantush (2006)	Comparison of KINEROS2 and GSSHA models for runoff and sediment loss estimation
The impact of parameter lumping and geometric simplification in modelling runoff and erosion in the shrublands of southeast Arizona	Canfield and Goodrich (2006)	Examining the impact of lumping and geometric simplification on model input parameters, simulated runoff volume and peak, sediment loss from hillslopes and channels on a small watershed in a semiarid rangeland
The Automated Geospatial Watershed Assessment (AGWA) Tool	Miller et al. (2007)	Developing a GIS based toolkit (AGWA) in ArcView GIS platform to fully parameterize, execute and visualize results from two distributed hydrological models, *i.e.,* Soil and Water Assessment Tool (SWAT) and Kinematic Runoff and Erosion Model (KINEROS2)
Application of the KINEROS2 rainfall-runoff model to an arid catchment in Oman	Al-Qurashi et al. (2008)	Identify optimal input parameters affecting modeling outputs, testing parameter estimation and its uncertainties towards predictions and comparing results with those achievable using simple empirical analysis
Understanding uncertainty in distributed flash flood forecasting for semiarid regions	Yatheendradas et al. (2008)	Evaluating the uncertainties towards input data sources to rainfall estimates, model parameters and initial soil moisture conditions in distributed flash flood forecasting for semiarid regions (high predictive uncertainty observed in the model response due to biases in the radar rainfall depth estimates; predictive performance of the model more influenced by real-time parameters rather than historical data)
KINEROS2/AGWA: Model use, calibration and validation	Goodrich et al. (2012)	Comprehensive review of KINEROS2 and AGWA with detailed reviews of prior studies (supported with few case studies on comparison of lumped to stepwise calibration/validation of runoff and sediment loss at plot, hill-slope and small watershed scales along with understanding of watershed response to wildfires using uncalibrated parameters
Risk assessment of post-wildfire hydrological response in semiarid basins: the effects of varying rainfall representations in the KINEROS2/AGWA model	Sidman et al. (2016)	KINEROS2/AGWA model was used to compare Pre and post fire rainfall-runoff events to determine the effect of differing representation on modeled peak flow and identify risk locations in semiarid basins
The paradoxical evolution of runoff in the pastoral Sahel: analysis of the hydrological changes over the Agoufou watershed (Mali) using the KINEROS-2 model	Gal et al. (2017)	KINEROS-2 model was used to compare rainfall-runoff events of past and present scenarios in Mali thus resulted into significant increase in annual discharge which is due to change in soil and vegetation cover

Table 3 (continued)

Title of study	References	Objectives of the study
KINEROS2-based simulation of total nitrogen loss on slopes under rainfall events	An et al. (2019)	The nutrient transport, runoff and sediment yield was modeled using KINEROS2 at runoff plot scale in the arid and semiarid regions of China

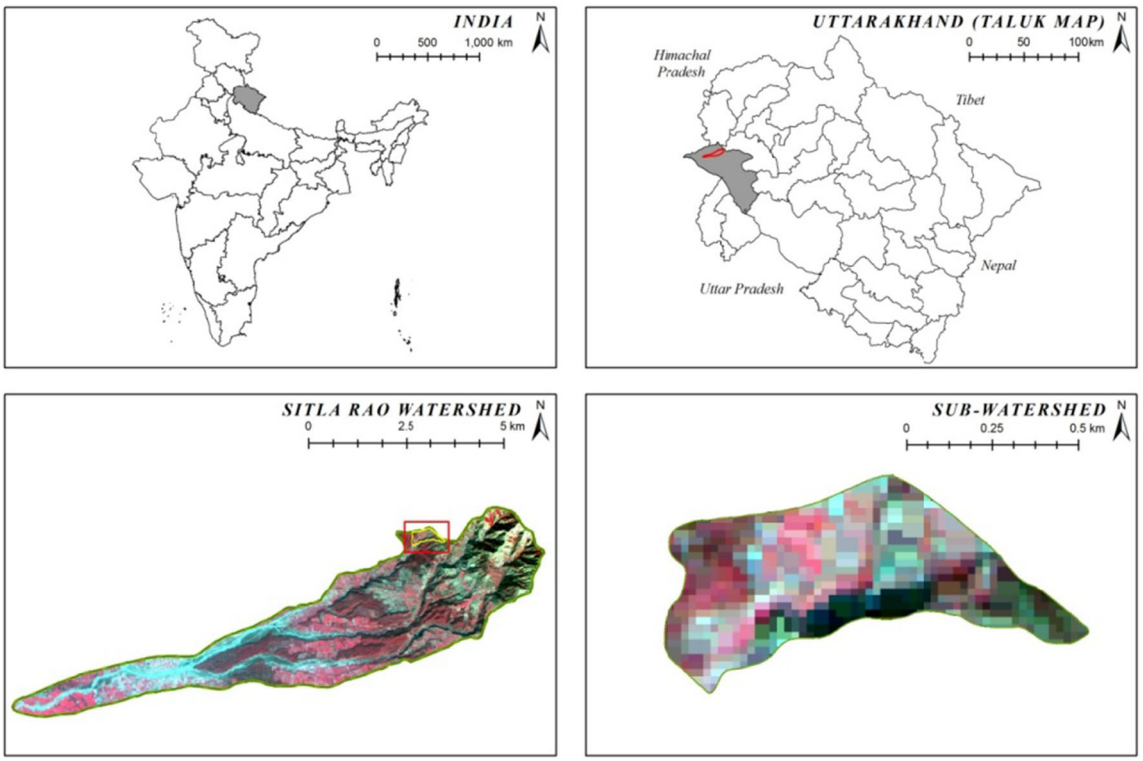

Fig. 1 Location map of the study area. The study site for hydrological modeling forms a sub-watershed (bottom right) of Sitla Rao watershed (bottom left)

Table 4 Rainfall Events and corresponding runoff used in model calibration and validation

Rain event	Date	Duration (min)	Rainfall (mm)	Observed runoff (mm/h)
E1	28.07.2003	144	58	20.16
E2	31.07.2003	678	27	1.76
E3	03.08.2003	45	25	7.16
E4	05.08.2003	113	17	1.98
E5	11.08.2003	203	36.2	11.07
E6	16.08.2003	30	25	6.03
E7	28.08.2003	59	40.5	10.78

bare condition with no vegetation during the sampling period.

The composite of five soil samples were obtained from each sampling site for soil moisture sampling. The depth interval taken for these soil samples was 0–5 cm, conforming to the microwaves penetration depth (Beven 2012; Srivastava et al. 2003). The soil samples were dried at 105^0 C for 24 h and weighed in two sets i.e., before and after drying and then, the gravimetric soil moisture content

Table 5 Details of ENVISAT ASAR data used for soil moisture estimation

Swath	Latitude	Longitude	Polarization	Acquisition date & time (h)	Pass	Orbit	Track
IS-6	30.43 N	78.01 E	VV and VH	06-June-2006, 04:43	D	22303	205
IS-4	30.43 N	77.95 E	VV and VH	09-June-2006, 04:49	D	22346	248
IS-2	30.38 N	78.26 E	VV and VH	12-June-2006, 04:54	D	22389	291

D Descending pass

was determined. The volumetric soil moisture *(θ)* is estimated by the following equation:

$$\theta = \left[\frac{w_{wet} - w_{dry}}{w_{dry}}\right]\frac{\rho_b}{\rho_w} \tag{4}$$

where w_{dry} is dried samples weight, w_{wet} is the weight of samples before drying, ρ_b is the dry bulk density and ρ_w is the water density. The dry bulk density of the soil samples was measured by 100 cm^3 ring samples filled with undisturbed soil after drying them for 24 h at 105 °C.

The surface roughness is measured using a pin profilometer having a length of 1 m with 2 cm sampling interval (Baghdadi et al. 2002). The three sets of roughness were taken for each sampling site and then, surface height's root mean square (RMS) was calculated by Eq. 5 (Gupta and Kapoor 2003):

$$RMS_{height} = \sqrt{\frac{1}{n_1 + n_2 + n_3}\left[n_1\left(\sigma_1^2 + d_1^2\right) + n_2\left(\sigma_2^2 + d_2^2\right) + n_3\left(\sigma_3^2 + d_3^2\right)\right]} \tag{5}$$

where σ^2 is the variance of all three surface roughness profiles as σ_1^2, σ_2^2,σ_3^2 and,

inferred that gives mean for all the three profiles of surface roughness (Eq. 6), and is the mean for every one of the three sets (*i.e.,* i = 1, 2, 3) of surface roughness profiles.

$$\overline{X} = \frac{n_1\overline{x}_1 + n_2\overline{x}_2 + n_3\overline{x}_3}{n_1 + n_2 + n_3} \tag{6}$$

where n_1, n_2 and n_3 refer to the total observations for all three profiles.

Model Parameterization Using Remote Sensing

Land-Use/Land-Cover

The LULC map of the Sitla Rao watershed was prepared utilizing microwave and optical remote sensing datasets. At first, two methodologies of digital image classification such as *decision tree* and *maximum likelihood classifier* (MLC) were applied, and the outcomes attained from the decision tree were enhanced and even better afterward post-classification sorting (Saran et al. 2007). The obtained LULC map, in any case, was not sufficient to utilize it as a model contributions, since two major crops, *i.e.,* maize and paddy, could not be discriminated. Consequently, we embraced a visual classification as an interactive approach by utilizing optical data and intertwined this with the ENVISAT ASAR data. The second step of comprehensive LULC classes (Fig. 2) resulted into the 'agricultural land' class with a higher classification accuracy. For further details on usage of satellite imagery and their results used, please see Saran et al. (2007, 2009).

Soil Moisture

The soil moisture is the impermanent water storage within the shallow layer of the earth's upper surface that helps in controlling all the agricultural activities and acts as a connection to balance energy and water at the land surface. The spatio-temporal behavioral data of near-surface soil moisture are essential elements both at global, regional and local scales. For the estimation of near-surface effective soil moisture, the microwave remote sensing has the advantages over conventional point observations in terms of large area coverage, repeatability and representation as area averages. The vital factor behind implementing the microwave remote sensing is the huge difference between dielectric water constant (approx.. 80) and dry soil (3 to 4) at microwave frequencies (Ulaby et al. 1986) which makes radar backscatter quite useful for soil moisture estimation.

The ENVISAT ASAR data of alternate polarization modes and numerous incidence angles were used for soil moisture assessment (Saran et al. 2014). The empirical models were produced for the evaluation of near-surface soil moisture through the alternate polarization ASAR data in exposed agricultural fields. As discussed in previous section, when the satellite passes, the ground measurement of surface roughness and soil moisture was achieved. Backscatter from vertical–vertical (VV) polarization signal and medium incidence angle (IS-4) was linked better with volumetric soil moisture content compared with other incidence angles. The model parameters were additionally improved and soil moisture estimation was refined by combining medium incidence angle (IS4) and vertical-horizontal (VH) polarization response as another variable along with VV polarization response (Saran et al. 2014). The local incidence angles, ASTER DEM derived, were incorporated to minimize the slope's effect on the radar backscatter. A spatially distributed map of near-surface soil moisture in plain agricultural fields was generated through

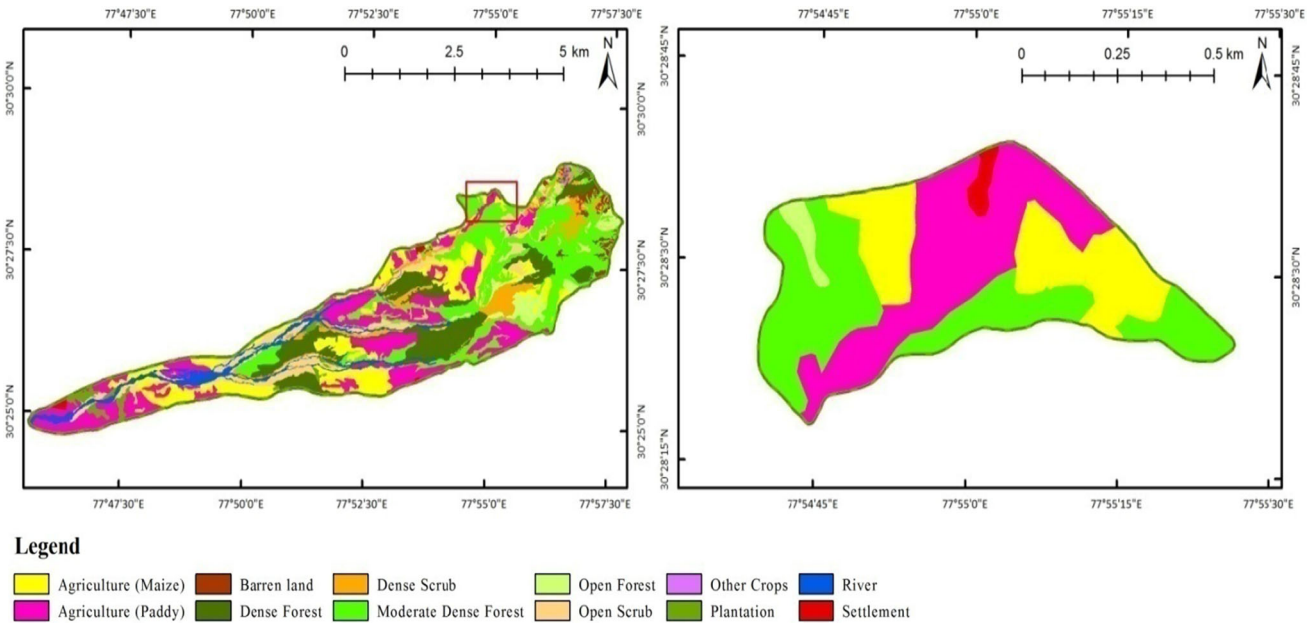

Fig. 2 Land-use/ land-cover map of Sitla Rao watershed (left) and sub-watershed (right) prepared using remote sensing data

this approach indicating that it ranges between 0.6% and 13% in the study area during the pre-monsoon period. These estimates have been used in KINEROS2 model to set the initial value of soil moisture for all the events.

Digital Elevation Models

Digital elevation models (DEMs) were derived from various sources, viz. high-resolution satellite stereo pairs from two stereo-imaging optical satellite sensors such as ASTER and CARTOSAT-1 PAN, topographic map at 1:50,000 scale, and SRTM (S*huttle Radar topographic mission*) (Saran et al. 2010). It was found in the previous study (Saran et al. 2010) that satellite derived DEM obtained from CARTOSAT-1 stereo-pair with 2.5 m spatial resolution provides highest vertical accuracy compared to other DEMs, as shown in Fig. 3. Here, the steps to generate DEMs from stereo images of CARTOSAT-1 are briefed because the DEM generation method is already published in Goncalves and Oliveira (2004).

The DEM was produced using *stereo analyst* function in ERDAS Imagine software from CARTOSAT-1 stereo-pair. The rational polynomial coefficients (RCP) were given for the two CARTOSAT images—*aft* and *fore*. Through triangulation, while using GCPs, the exterior orientation parameters were refined and the tie points were obtained to measure the coordinate positions of images from ground points which appeared on overlying part of above-mentioned scenes. After triangulation approach, the DEM was generated with 4.5 m vertical accuracy.

Delineation of Hydrologic Response Units (HRUs)

HRUs representing the same zones which are susceptible to different degrees of surface soil erosion and runoff, were distinguished to produce the velocity of surface runoff based on their potential. The initial condition (runoff potential) is correlated to the volume of surface runoff, whereas the next condition (velocity of runoff) is associated to the soil detachment capacity. The HRUs were delineated using LULC, soil depth, and slope derived from the CARTOSAT DEM (Saran et al. 2010). The spatial distribution of HRUs in the Sitla Rao watershed is shown in Fig. 4.

The descriptions of individual HRUs are given below:

HRU-1 This hydrological unit is useful for those areas which are fully terraced and are puddled prior to rice transplant. In this way, it brings the ponding of water in the field and surface runoff begins once the fields are filled with water and streams over the bund into the next paddy field or river. They are mainly circulated in the upper and the center part of the watershed. This HRU signifies the zone with no immediate surface runoff generation, though the deposition of sediments may occur due to negligible flow velocities. Such unit is unique in its behavior because of the controlled erosion-reducing practices.

HRU-2 This unit is for the areas which are covered with moderate to high densities of forest with deep soil and high infiltration capacity. The HRU-2 is chiefly confined to the lower piedmont physiographic unit with gentle slopes (0–6%). The hydrological behavior represents very high infiltration and lowest surface runoff potential.

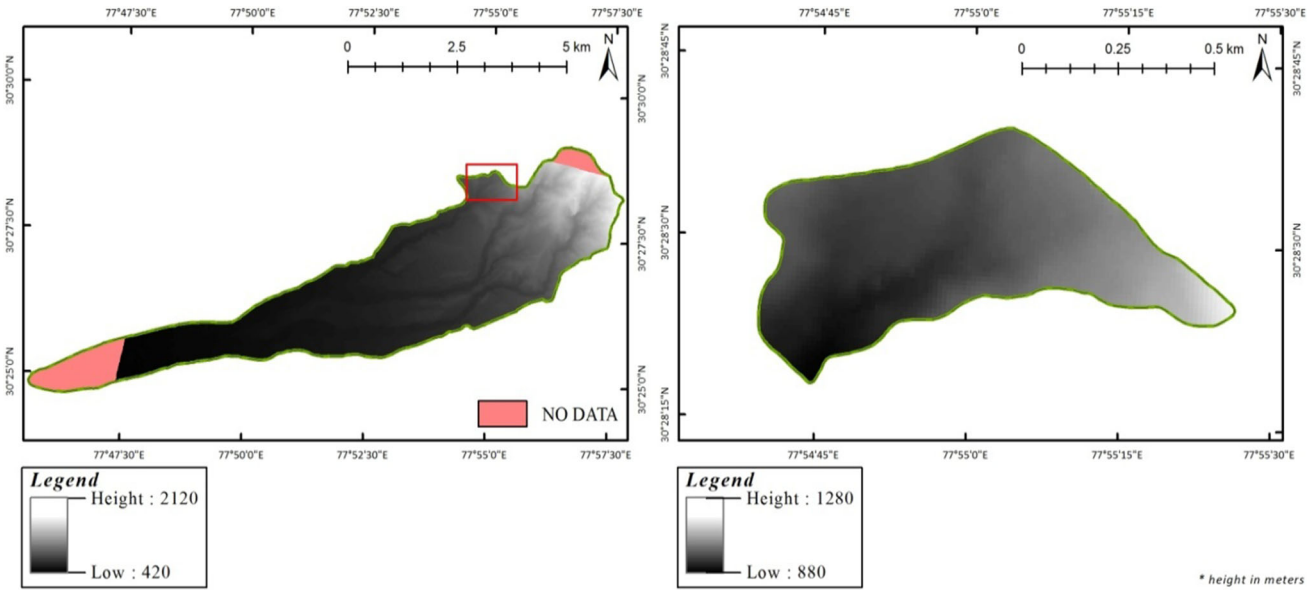

Fig. 3 Digital elevation model (DEM) of Sitla Rao watershed (left) and sub-watershed (right) derived from CARTOSAT-1 data

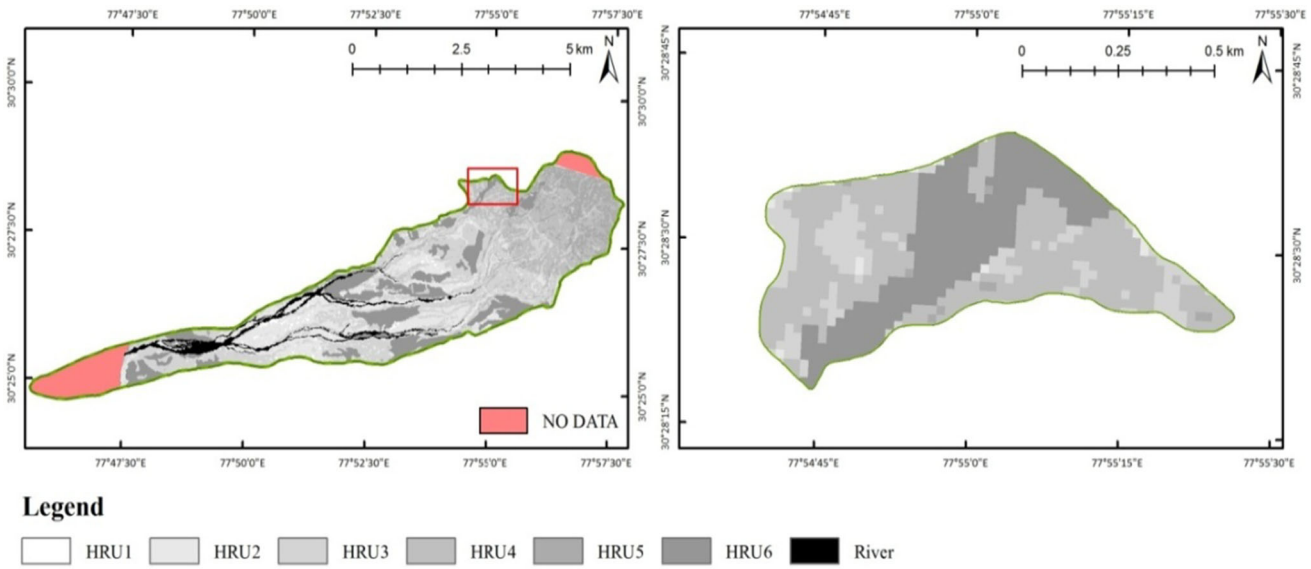

Fig. 4 HRU map of Sitla Rao watershed (left) and sub-watershed (right)

HRU-3 This spatial unit comprises the upper piedmont physiographic unit with undulating slopes (6–15%) of those areas with dense, open and degraded forest cover. As such forest cover, the capture of rainfall is high that leads in reduction of the surface runoff. The soil is deep with high effective hydraulic depth and good infiltration capacity. This HRU represents the zone with low surface runoff generation and erosion.

HRU-4 The hydrological behavior of this unit represents moderate infiltration capacity with moderate surface runoff generation. The soil depth is moderate to shallow with moderate effective hydrological depth. This is confined to middle elevation zones with moderate slopes (16–30%). The major LULC is dense and open scrub.

HRU-5 The hydrological behavior of this unit represents the infiltration range from moderate to low and a relatively high surface runoff generation. The soil depth is shallow with low effective hydrological depth and low infiltration capacity. This unit is confined to middle elevation zones which are having relatively steeper slopes (31–45%). The major LULC classes are agriculture (maize), barren land and settlement.

HRU-6 This spatial and homogenous unit is confined to high elevation zones of the watershed, having steep slopes

(> 45%). Also, the soil depth is shallow and effective hydrological depth is small and the main LULC classes are barren land, agriculture (maize) and settlement. In this, the infiltration capacity is low and thus, high surface runoff is expected. This HRU depicts the zone with maximum surface runoff and a high erosion potential.

Model Calibration, Validation and Performance Testing

Model Calibration and Validation

The calibration and validation of model are an important phases in developing and implementing the process-based hydrological models. While calibration is an iterative methodology for evaluating and refining parameter by comparing it with the simulated and observed values of interest. Then the validation is proceeded to guarantee that the calibrated model appropriately evaluates all conditions and variables that may influence model outcomes and determines the ability to forecast field observations for periods not the same as that utilized in the calibration process.

In this study, we have used three variables for calibrating the model, *i.e.,* saturated hydraulic conductivity, Manning's coefficient and initial soil moisture, which have significant influence on surface the runoff generation (Al-Qurashi et al. 2008; Yatheendradas et al. 2008). The calibration is performed on four rainfall events (E1, E2, E3 and E5). Once the parameters are optimized, validation is performed on remaining three rainfall events (E4, E6 and E7) and overall performance of the model is assessed.

Model Performance

The model performance is evaluated using two methods: *root mean square error* (RMSE) and Nash–Sutcliffe coefficient (E). The RMSE is expressed as:

$$RMSE = \sqrt{\frac{\sum_{i=1}^{N} (P_i - O_i)^2}{N}} \tag{7}$$

where P_i represents the model estimated value of runoff, O_i is the observed runoff and N demotes total observations, here N is four.

The Nash–Sutcliffe model efficiency coefficient is one of the commonly known methods used to evaluate hydrological model behavior through comparisons of simulated and observed runoff (Nash and Sutcliffe, 1970). It is given as:

$$E = 1 - \frac{\sum_{i=0}^{n} (O_i - P_i)^2}{\sum_{i=0}^{n} (O_i - \overline{O})^2} \tag{8}$$

where O_i is observed discharge, P_i *is* predicted discharge and $\overline{O}$ is the mean of observed discharge. The value of E can range from $-\infty$ to 1. An efficiency of 1 (E = 1) corresponds to a perfect match of modeled discharge to the observed data. An efficiency of 0 (E = 0) indicates that the model predictions are as accurate as the mean of the observed data, whereas an efficiency less than zero (E < 0) occurs when the observed mean is a better predictor than the model. Therefore, the closer the E value is to 1, the more accurate the model is (Moriasi et al. 2007).

Results and Discussion

Watershed Delineation and Discretization Using AGWA

Watershed delineation and discretization is a process to extract stream network by computing gathered area upslope of each pixel through a network of cell-to-cell drainage paths. The catchment of modeled site (sub-watershed of Sitla Rao watershed) has been delineated and discretized using AGWA tool in ArcGIS software (version 9.2) for setting up the KINEROS2 model. CARTOSAT-1 DEM was used as input for this. The watershed is subdivided into planes and channels depending upon the stream network density. The user-defined locations of internal gauges either locations where model output is required for model calibration and validation or discharge gauging stations, split watershed along with channel network. Thus, the channel network is considered by various hydraulic-geometry or by a user-defined relations with areas contributing to channel geometry (Semmens et al. 2008). The slope of the individual plane is valued as per the average plane slope; whereas, the geometric characteristics such as plane width and length are a function of the plane shape assuming a rectangular shape where the longest flow length is equal to element length (Semmens et al. 2008). The geometric characteristics of channels are parameterized following Miller et al. (2007). However, all channels are considered as uniform except those which are related to soil characteristics and thus, these exceptions are assumed as sandy bed. The DEM derived slope grid determines the channel slope (Semmens et al. 2008). The schematic representation of watershed discretization is shown in Fig. 5. The modeled watershed is divided into 51 planes and 21 channels of different geometry. The channel number 23 is an outlet where runoff has been recorded. The runoff in each channel is contribution of adjacent/connected planes

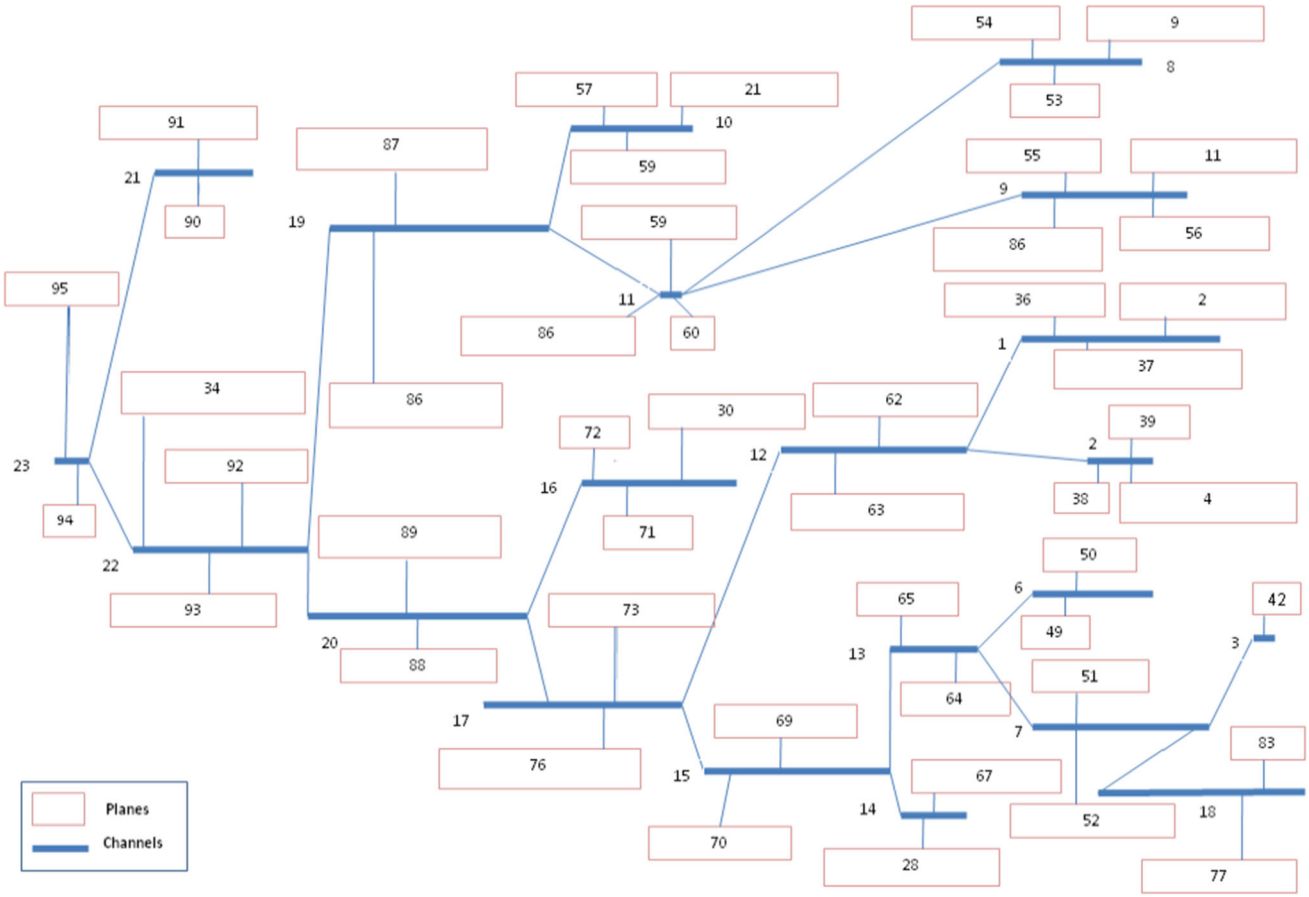

Fig. 5 Model schematic of watershed discretization into planes and channels. Numbers indicated on the planes and channels are ID numbers generated by the software

and is also further linked to different streams depending upon the hierarchy.

The spatial depiction of planes and channel network at the modeled site is shown in Fig. 6, and their geometry (length, width and slope) is given in Table 6.

Model Parameterization

Three spatial layers, viz. soil, LULC and topography (DEM) have been used for model parameterization. The discretized planes and channels (please see Sect. 4.1) were

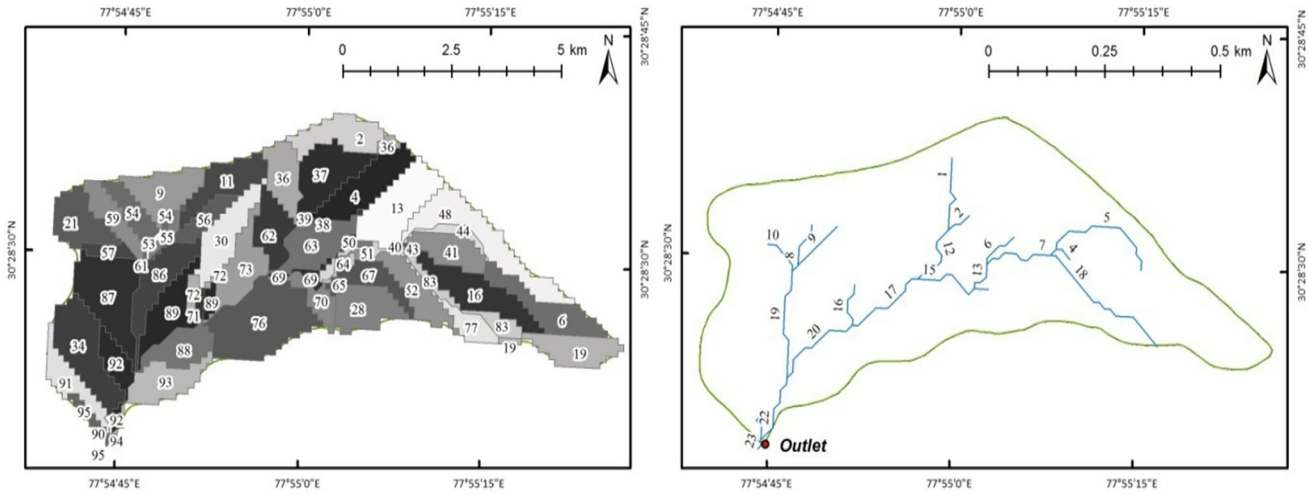

Fig. 6 Planes and channel network with discharge outlet for modeled catchment

Table 6 Geometry of discretized planes and channels

Geometry of planes and channels	Planes (n = 51)			Channels (n = 21)		
	Maximum (m)	Minimum(m)	Average (m)	Maximum (m)	Minimum (m)	Average (m)
Length	313.64	17.67	113.69	313.64	17.67	118.75
Width	498.28	5.17	88.60	10	3	7
Slope (fractional rise/run)	0.585	0.003	0.314	0.437	0.003	0.217

intersected with soil and LULC maps for the extraction of attributes from the respective lookup tables. The individual planes or overland elements are in the form of spatially lumped units which perform uniformly within a given element in spite of spatial variability with respect to topography, soil and LULC. Series of GIS spatial analysis operations were performed for parameter estimation. The value for each parameter within the plane and channel were estimated using area-weighting scheme of AGWA tool (Miller et al. 2007).

The parameters such as rock fraction, suction head, porosity, saturated hydraulic conductivity associated with corresponding soil texture were taken from the existing lookup tables (Woolhiser et al. 1990; Rawls et al. 1982) and manually edited in the attribute table of planes and channels. The LULC parameters which includes interception, Manning's roughness, canopy cover and percent paved area have been taken from the published literature available as lookup tables (Woolhiser et al. 1990) in AGWA. The values of different parameters for planes and channels are given in Table 7. The initial soil moisture value for all the events is taken as 0.138 (default value by the model) to initialize the model run.

After discretization, delineation and parameter estimation of planes and channels, all the data were converted into parameter file following the order of channels and corresponding contributing planes. This file has been prepared manually in Microsoft WordPad to run KINEROS2 model. Overall, seven parameter files have been prepared corresponding to rainfall events.

Runoff Modeling

The model was run on all the seven rainfall events of different intensities classified into very heavy, heavy, moderate and light events using the initial parameter values (Table 7). The rainfall events pertain to July and August, 2003 and are selected as the measured runoff values are available for these events. The results of uncalibrated model run are shown in Table 8. The model in general performed well for all rainfall events. However, the performance was better for bigger (higher intensity) rain storms compared to smaller ones. Further, it is observed that the model in general overestimates the runoff for longer duration rain events and underestimates for shorter duration rain events. Since the model is influenced by many parameters like saturated hydraulic conductivity, Manning's coefficient, initial soil moisture, intercepted depth, etc., it is necessary to identify the most sensitive parameter(s) influencing the modeling results. Therefore,

Table 7 Parameter values used in KINEROS2 model for the study site

Parameter	Symbol	Units	Value/range (planes)	Value/range (channels)
Manning Coefficient	n	$sm^{-1/3}$	0.065	0.042
Saturated hydraulic conductivity	K_s	mm/h	1.05–24.40*	10.998
Capillary length scale	G	mm	84.54–288.16	2.21
Variation of K_s	CV	–	0.42–1.02	NA
Initial Saturation	SAT	–	–	0.2
Pore size distribution index	d	–	0.11–0.28	0.8
Soil porosity	Θ	–	0.22–0.59	0.437
Interception depth	i	mm	0.5–4.0	NA
Rock cover	r	–	0.03–0.41	0
Plant Cover	p	–	0.5	NA
Splash	s	–	47.08–122.38	NA
Cohesion	c	–	0.002–0.007	0.01

*Majority planes have value ranging from 1 to 8 mm/h, very few planes have values > 15

Table 8 Results of uncalibrated model run for different rain events

Rainfall events	Rainfall duration (minutes)	Rainfall intensity (mm/h)	Intensity classified events	Observed runoff (mm/h)	Modeled runoff (mm/hr)
E1	144	24.16	Heavy	20.16	24.37
E2	678	2.38	Light	1.76	0.12
E3	45	33.33	Very heavy	7.16	3.42
E4	113	9.02	Moderate	1.98	0.7
E5	203	10.69	Moderate	11.07	11.28
E6	30	50	Very heavy	6.03	5.1
E7	59	41.18	Very heavy	10.78	11.64

first the sensitivity analysis was carried out, followed by model calibration and validation.

Sensitivity Analysis

The degree of effect which is on the output by model's parameter is determined by the sensitivity analysis and hence, the number of parameters required in calibration get reduced. Three most important parameters, affecting the runoff have been considered for this purpose. They are: saturated hydraulic conductivity (K_s), Manning's coefficient (n) and initial soil moisture (SAT) (Al-Qurashi et al. 2008; Yatheendradas et al. 2008). For sensitivity analysis, the value of one parameter will change, while others two will remain constant at their initial values (Table 7). The results are shown in Fig. 7. It is observed that increasing the K_s and n values result in lowering the modeled runoff, while it is vice versa in case of SAT. Further, K_s is the most sensitive parameter compared to n and SAT as the modeled runoff changes significantly (high slope) with the change in K_s for all the rain events. Therefore, it is obvious that K_s has to be calibrated more precisely and effectively for preparing a robust model and better estimation of surface runoff.

Model Calibration and Validation

The model calibration is carried out using four rain events of different intensities, *i.e.,* light, moderate, heavy and very heavy rain events (E1, E2, E3 and E5). The calibration is done in two stages. In the first stage, the value of K_s, n and SAT is changed from − 30% to + 30% of the initial value at interval of 5% and RMSE is estimated for each model run. While changing the value of one parameter, the other two parameters are kept at initial values. This step helped in finding the initial calibrated values for three parameters (K_s, n, and SAT). In the second stage, n and SAT values are changed to the calibrated values obtained during the first step and the value of K_s, being the most sensitive parameter, was optimized by evaluating the model results based on RMSE and Nash–Sutcliffe model efficiency coefficient. The details are discussed in following paragraphs.

Table 9 presents the results of the first stage of calibration. The initial SAT value is taken as 0.138 (please see Sect. 4.2), therefore, its calibration range varied from 0.0966 (− 30% or 0.7 times of the initial value) to 0.1794 (+ 30% or 1.3 times of the initial value). Similarly, the initial values of K_s and n are also varied from − 30% to + 30% of the initial values (please see Table 7 for initial values). The RMSE values obtained after each model run reveal that the K_s value is close to + 25% of the initial value, and n and SAT values are close to − 30% of their respective initial values. It is observed from Table 9 that even if the SAT value is changed from 0.138 (initial value) to 0.0966 (− 30% of the initial value), RMSE changes by 0.04. In other words, the effect of variation in SAT value on modeled runoff is not significant. The soil moisture values estimated from ENVISAT ASAR data pertaining to pre-monsoon season ranges from 0.06 to 0.13 (Saran et al. 2014). Since the rain events being modeled in the present study pertain to monsoon season, hence the maximum soil moisture value of 0.13 estimated from ENVISAT ASAR data is considered as the appropriate SAT value in the model. Also, it is observed from Table 9 that change in RMSE is only 0.02 if the initial SAT value is changed from − 5% to − 30%. The value of n is fixed as 0.70 (*i.e.,* − 30% of the initial value). As K_s is the most sensitive parameter (Fig. 7 and Table 9) and also that it has a considerable variability in the study area (1.05 to 24.4 mm/hr, majority values lie between 1 and 8 mm/hr), its value is fine-tuned during the second stage of calibration while fixing the values of n and SAT as 0.70 and 0.13.

Table 10 presents the results of the second stage of calibration. The model performance is evaluated based on RMSE as well as Nash–Sutcliffe model efficiency coefficient (E). The results of model run indicate that K_s value

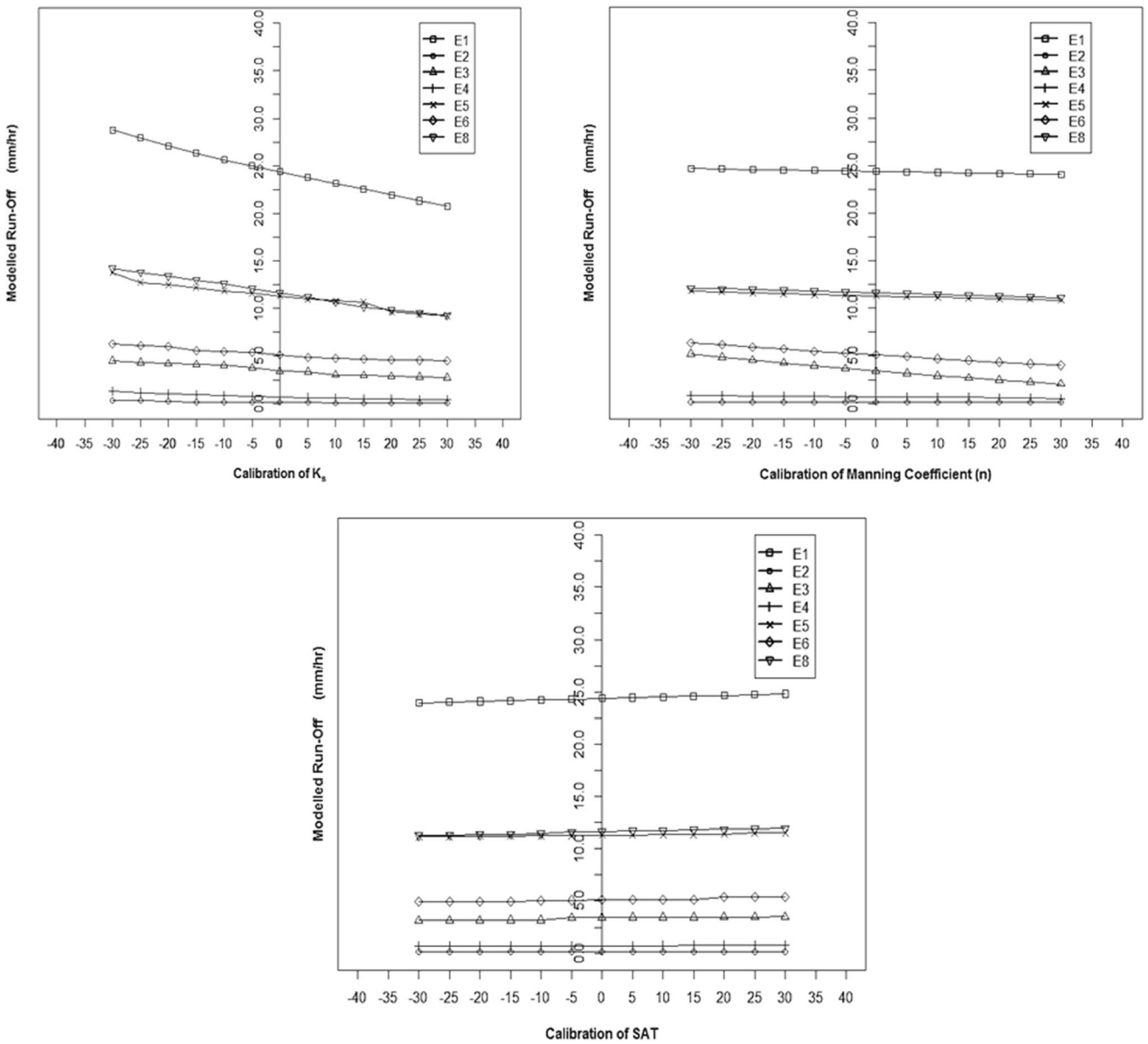

Fig. 7 Modeled runoff (y-axis) as a result of changing the saturated hydraulic conductivity (top left), Manning coefficient (top right), and initial soil moisture (bottom left). While changing one parameter, other two parameters are kept at initial values (Table 7)

Table 9 RMSE estimate for first stage of calibration (four rain events E1, E2, E3 and E5 are used)

Parameters	− 30%	− 25%	− 20%	− 15%	− 10%	− 5%	0	5%	10%	15%	20%	25%	30%
K_s	3.60	3.24	2.96	2.70	2.48	2.33	2.22	2.08	2.03	1.94	1.94	**1.93***	1.94
N	**1.98***	2.01	2.04	2.08	2.12	2.17	2.22	2.27	2.32	2.36	2.41	2.46	2.51
SAT	**2.18***	2.20	2.21	2.23	2.24	2.20	2.22	2.23	2.25	2.27	2.29	2.31	2.33

*Most significant

can be optimized as + 30% (or 1.30 times) of the initial value.

Model validation is carried out using the remaining three rain events of moderate and very heavy intensity (E4, E6 and E7) and taking the calibrated values of K_s, n and SAT. The Nash–Sutcliffe model efficiency coefficient was obtained as 0.906 and the RMSE as 1.097 (Table 11). These values indicate that the parameterization and

Table 10 Model evaluation by calibrating K_s value while fixing n = 0.70 and SAT = 0.13 during the second stage of calibration

Rain event	Rain intensity	1%	5%	10%	20%	30%	35%	40%	50%
E1	Heavy	24.493	24.017	23.495	22.194	21.039	20.495	19.904	18.959
E2	Light	0.137	0.125	0.109	0.076	0.057	0.047	0.042	0.0284
E3	Very heavy	5.175	5.092	4.738	4.522	4.339	4.25	4.138	3.978
E5	Moderate	11.769	11.523	11.388	10.13	9.745	9.351	9.202	8.913
RMSE		2.54	2.34	2.22	1.92	1.82*	1.90	1.97	2.19
Nash–Sutcliffe coefficient		0.908	0.921	0.929	0.947	**0.952***	0.948	0.944	0.931

*Most significant

calibration is indicative of the hydrological behavior of the watershed in terms of runoff.

Validation of Hydrologic Response Units

Hydrologic response units (HRUs) provide qualitative runoff potential, while KINEROS2 model provides quantitative runoff in the discretized planes. The HRUs delineated in the previous research study (Saran et al. 2010) are validated with the results obtained from KINEROS2 model. For this purpose, the discretized model domain consisting of planes and channels were overlaid on HRUs map to derive the composition of planes in individual HRUs. Of the six HRUs in Sitla Rao watershed, only four HRUs fall within the model domain (HRU-1, 3, 4, and 5).

Table 12 provides the details of representative KINEROS2 discretized planes for each HRU and the modeled runoff. The KINEROS2 planes are considered to be the representative of HRUs if the full or major portion of the planes lie within the HRUs. Planes 53, 56, 88 fall completely within the HRUs, while the remaining planes (21, 36, 62, 63, 70, 86, 87 and 89) have major portions within the HRUs. None of the planes completely lie in HRU-5 and hence it is represented by the plane (70) having its dominant part within it. The KINEROS2 model is run for best representative planes lying in different HRUs (plane 88 in HRU-1; plane 53 in HRU-3; plane 56 in HRU-4; plane 70 in HRU-5) for estimating the runoff, shown in Table 12. As mentioned earlier in Sect. 3.3.4, the HRUs showing qualitative runoff potential were derived from LULC, soil depth and slope using GIS-based overlay approach. Whereas, process-based KINEROS2 model uses DEM (topography) for discretization of the area and then appends parameters (or attributes) to the discretized planes and channels on the basis of LULC and soil maps. The comparison of runoff potential of HRUs with the corresponding KINEROS2 modeled runoff (Table 12) shows similar pattern, thereby validating the HRUs delineated in the study area in a previous study. This indicates that remote sensing and GIS-based HRUs can be used as good surrogate for assessing the runoff potential where quantitative runoff measurements are unavailable. Further, such qualitative assessments through HRUs are especially useful in spatially discretizing the study watershed into different runoff potential units, which can prove to be of immense value in taking up appropriate watershed management practices.

Discussion

In this study, remote sensing has been used to its maximum potential for providing basic inputs and parameterization of KINEROS2 model in terms of topography, LULC and near-surface soil moisture. The DEM derived from high-resolution remote sensing data formed the basic input to KINEROS2 model for discretizing the model domain into a mosaic of planes and channels. The LULC map is used to derive Manning's coefficient (n), interception, plant canopy cover. The near-surface soil moisture map derived from microwave remote sensing data is used to initialize soil moisture (SAT) parameter during model run for different rain events. All these remote sensing derived datasets in conjunction with field data have been integrated in GIS domain to perform spatially distributed KINEROS2 modeling. GIS tool (AGWA) helped to store watershed data and to further interact with KINEROS2 model in

Table 11 Validation of model using three rain events

Rain event	Intensity	Observed runoff (mm/h)	Simulated runoff (mm/h)
E4	Moderate	1.98	0.49
E6	Very heavy	6.03	5.708
E7	Very heavy	10.78	9.644
RMSE			1.097
Nash–Sutcliffe model efficiency coefficient			0.906

Table 12 Validation of HRUs with KINEROS2-based discretized planes for runoff estimation

HRUs and their runoff potential			KINEROS2 discretized planes and modeled runoff		
HRU	Majority land-use/land-cover	Runoff potential	Nos. of representative planes	Planes with IDs	Modeled runoff (mm/h)
HRU 1	Paddy	Low runoff	4	36, 62, 63, 88*	0.35
HRU 3	Dense Forest	Medium runoff	3	21, 53*, 86	2.43
HRU 5	Mod. Dense forest	High Runoff	1	70* (majority)	9.91
HRU 4	Maize	High Runoff	3	56*, 87, 89	11.46

*Individual planes representative of HRUs on which KINEROS2 model is run to estimate runoff

setting up model runs and displaying the results. In a rugged and poorly accessible terrain like Himalaya which are also data scarce, remote sensing can prove to be a vital tool for parameterizing the hydrological and soil erosion models like KINEROS2.

It is observed that KINEROS2 model in general performed well for all rain events having different intensities, ranging from light to very heavy (Table 8). However, the performance was better for bigger (higher intensity) rain storms compared to small rain storms. Further, the model overestimated the runoff for longer rainfall duration and vice versa. Like previous studies (e.g., Yatheendradas et al. 2008; Goodrich et al. 2012), the present study also indicates that the most sensitive hill-slope parameter influencing the surface runoff is saturated hydraulic conductivity of soil, followed by Manning's coefficient and initial soil moisture. Since the model has been calibrated and validated for rain events of light to very heavy intensity, it can be used to perform runoff predictions for variable intensity rain events. The model may also be used to understand the implications of future climate on the runoff and sediment loss from the watershed.

There are a few limitations in the present study. The total number of rain events (seven nos.) used for running the KINEROS2 model is quite less. This limitation could not be overcome as the runoff data were available only for these events. The availability of hydrograph, instead of total (single value) runoff data, and the sediment loss data would have resulted in better calibration and validation of the model. Similarly, the availability of microwave and optical remote sensing data concurrent with the rain events would have also improved the model parameterization and initialization.

Conclusions

The present study couples remote sensing, GIS and KINEROS2 model in a Himalayan watershed for spatially distributed runoff modeling. Optical and microwave remote sensing data are primarily used for model parameterization, *i.e.,* characterizing the individual planes and channels in terms of topography, LULC and near-surface soil moisture using. Customized GIS tool, AGWA, helped in storing, manipulation, analysis and visualization of watershed data and results. The KINEROS2 model in general performs well in a small Himalayan watershed. The model performance is found to be better for higher intensity rain events compared to smaller ones. The model also overestimated the runoff for longer duration rain events and vice versa. Saturated soil hydraulic conductivity is the most sensitive parameter influencing the runoff compared to Manning's coefficient and initial soil moisture as reported in previous studies. The KINEROS2 estimated runoff is used for validating the remote sensing and GIS based HRUs delineated in a previous research study. This indicates that remote sensing and GIS-based HRUs can be used as good surrogate for assessing the qualitative runoff potential where quantitative runoff measurements are unavailable, especially in poorly accessible and data scarce areas like the Himalayan watersheds.

Despite limitations, the study highlights that the coupling of remote sensing and GIS with process models, such as KINEROS2, can provide valuable information in planning sustainable watershed management practices in the Himalayan watersheds. Since the model has been calibrated and validated for rain events of light to very heavy intensity, it can be used to perform runoff predictions for variable intensity rain events, including studies to understand the implications of future climate.

Acknowledgements Funding of this research was provided by SAIL GEONEDIS Project through IIRS & WU joint collaboration. The authors are thankful to Dr. S.K. Srivastav for his critical comments and suggestions in improving the manuscript. Also the help with soils data provided by Dr. Suresh Kumar is much appreciated.

References

Al-Qurashi, A., McIntyre, N., Wheater, H., & Unkrich, C. (2008). Application of the Kineros2 rainfall-runoff model to an arid

catchment in Oman. *Journal of Hydrology, 355*(1–4), 91–105. https://doi.org/10.1016/j.jhydrol.2008.03.022.

An, M., Han, Y., Xu, L., Wang, X., Ao, C., & Pang, D. (2019). KINEROS2-based simulation of total nitrogen loss on slopes under rainfall events. *CATENA, 177,* 13–21. https://doi.org/10.1016/j.catena.2019.01.039.

Baghdadi, N., King, C., Bourguignon, A., & Remond, A. (2002). Potential of ERS and Radarsat data for surface roughness monitoring over bare agricultural fields: Application to catchments in Northern France. *International Journal of Remote Sensing, 23*(17), 3427–4344. https://doi.org/10.1080/01431160110110974.

Band, L. E., & Moore, I. D. (1995). Scale: Landscape attributes and geographical information systems. *Hydrological Processes, 9*(3–4), 401–422. https://doi.org/10.1002/hyp.3360090312.

Beven, K. (2012). *Rainfall-runoff modelling*. London: Wiley.

Canfield, H. E., & Goodrich, D. C. (2006). The impact of parameter lumping and geometric simplification in modelling runoff and erosion in the shrublands of southeast Arizona. *Hydrological Processes, 20*(1), 17–35. https://doi.org/10.1002/hyp.5896.

Moriasi, D. N., Arnold, J. G., Van Liew, M. W., Bingner, R. L., Harmel, R. D., & Veith, T. L. (2007). Model evaluation guidelines for systematic quantification of accuracy in watershed simulations. *Transactions of the ASABE, 50*(3), 885–900. https://doi.org/10.13031/2013.23153.

Duru, J. O., & Hjelmfelt, A. T. (1994). Investigating prediction capability of HEC-1 and KINEROS kinematic wave runoff models. *Journal of Hydrology, 157*(1–4), 87–103. https://doi.org/10.1016/0022-1694(94)90100-7.

Entekhabi, D., Nakamura, H., & Njoku, E. G. (1994). Solving the inverse problem for soil moisture and temperature profiles by sequential assimilation of multifrequency remotely sensed observations. *IEEE Transactions on Geoscience and Remote Sensing, 32*(2), 438–448.

Famiglietti, J. S., & Wood, E. F. (1994). Multiscale modeling of spatially variable water and energy balance processes. *Water Resources Research, 30*(11), 3061–3078. https://doi.org/10.1029/94WR01498.

Flügel, W. A. (1997). Combining GIS with regional hydrological modelling using hydrological response units (HRUs): An application from Germany. *Mathematics and Computers in Simulation, 43*(3–6), 297–304. https://doi.org/10.1016/s0378-4754(97)00013-x.

Gal, L., Grippa, M., Hiernaux, P., Pons, L., & Kergoat, L. (2017). The paradoxical evolution of runoff in the pastoral Sahel: Analysis of the hydrological changes over the Agoufou watershed (Mali) using the KINEROS-2 model. *Hydrology and Earth System Sciences, 21*(9), 4591. https://doi.org/10.5194/hess-21-4591-2017.

Goncalves, J. A., & Oliveira, A. M. (2004). Accuracy analysis of DEMs derived from ASTER imagery. *International Archives of Photogrammetry and Remote Sensing, 35,* 168–172.

Goodrich, D. C., Burns, I. S., Unkrich, C. L., Semmens, D. J., Guertin, D. P., Hernandez, M., et al. (2012). KINEROS2/AGWA: Model use, calibration, and validation. *Transactions of the ASABE, 55*(4), 1561–1574.

Goodrich, D. C., Williams, D. G., Unkrich, C. L., Hogan, J. F., Scott, R. L., & Hultine, K. R., et al. (2013). Comparison of methods to estimate ephemeral channel recharge, Walnut Gulch, San Pedro River Basin, Arizona. In *Groundwater recharge in a desert environment: The Southwestern United States*. https://doi.org/https://doi.org/10.1029/009WSA06

Gupta, S. C., & Kapoor, V. K. (1970). *Fundamentals of mathematical statistics*. Delhi: Sultan Chand & Sons.

Jain, S. K., Kumar, S., & Varghese, J. (2001). Estimation of soil erosion for a Himalayan watershed using GIS technique. *Water Resources Management, 15*(1), 41–54. https://doi.org/10.1023/A:1012246029263.

Kalin, L., Govindaraju, R. S., & Hantush, M. M. (2003). Effect of geomorphologic resolution on modeling of runoff hydrograph and sedimentograph over small watersheds, *276*(1–4), 89–111. *Journal of Hydrology*. https://doi.org/10.1016/S0022-1694(03)00072-6.

Kalin, L., & Hantush, M. H. (2006). Comparative assessment of two distributed watershed models with application to a small watershed. *Hydrological Processes, 20*(11), 2285–2307. https://doi.org/10.1002/hyp.6063.

King, C. H., & Delpont, G. (1993). Spatial assessment of erosion: contribution of remote sensing, a review. *Remote Sensing Reviews, 7*(3–4), 223–232.

Kite, G. W. (1995). Scaling of input data for macroscale hydrologic modeling. *Water Resources Research, 7*(3–4), 223–232. https://doi.org/10.1029/95WR02102.

Michaud, J. D., & Sorooshian, S. (1994). Effect of rainfall-sampling errors on simulations of desert flash floods. *Water Resources Research, 30*(10), 2765–2775. https://doi.org/10.1029/94WR01273.

Miller, S. N., Semmens, D. J., Goodrich, D. C., Hernandez, M., Miller, R. C., Kepner, W. G., & Guertin, D. P. (2007). The automated geospatial watershed assessment tool. *Environmental Modelling and Software, 22*(3), 365–377. https://doi.org/10.1016/j.envsoft.2005.12.004.

Miller, S., & Semmens, D. (2002). GIS-based hydrologic modeling: the automated geospatial watershed assessment tool. In *Proceeding of the second federal interagency hydrologic modeling conference* (Vol. 28). Las Vegas Nevada.

Moore, I. D., Grayson, R. B., & Ladson, A. R. (1991). Digital terrain modelling: A review of hydrological, geomorphological, and biological applications. *Hydrological Processes, 5*(1), 3–30. https://doi.org/10.1002/hyp.3360050103.

Moore, I. D., Gessler, P. E., Nielsen, G. A., & Peterson, G. A. (1993). Soil attribute prediction using terrain analysis. *Soil Science Society of America Journal, 57*(2), 443–452. https://doi.org/10.2136/sssaj1993.03615995005700020058x.

Morgan, R. P. C. (2001). A simple approach to soil loss prediction: A revised Morgan-Morgan-Finney model. *CATENA, 44*(4), 305–322. https://doi.org/10.1016/S0341-8162(00)00171-5.

Morgan, R. P. C. (2005). Soil erosion and conservation. *Journal of Chemical Information and Modeling*.

Nash, J. E., & Sutcliffe, J. V. (1970). River flow forecasting through conceptual models part I - A discussion of principles. *Journal of Hydrology, 10*(3), 282–290. https://doi.org/10.1016/0022-1694(70)90255-6.

Parlange, J. Y., Lisle, I., Braddock, R. D., & Smith, R. E. (1982). The three-parameter infiltration equation. *Soil Science, 133*(6), 337–341. https://doi.org/10.1097/00010694-198206000-00001.

Quincey, D. J., Luckman, A., Hessel, R., Davies, R., Sankhayan, P. L., & Balla, M. K. (2007). Fine-resolution remote-sensing and modelling of Himalayan catchment sustainability. *Remote Sensing of Environment, 107*(3), 430–439. https://doi.org/10.1016/j.rse.2006.09.021.

Rawls, W. J., Brakensiek, C. L., & Saxton, K. E. (1982). Estimation of soil water properties. *Transactions - American Society of Agricultural Engineers, 25*(5), 1316–1320. https://doi.org/10.13031/2013.33720.

Rovey, E. W., Woolhiser, D. A., & Smith, R. E. (1977). *A distributed kinematic model of upland watersheds* (p. 52). *Colo State Univ (Fort Collins) Hydrol Pap*.

Saran, S., Sterk, G., & Kumar, S. (2007). Optimal land use/cover classification using remote sensing imagery for hydrological modelling in a Himalayan watershed. In *Remote sensing for agriculture, ecosystems, and hydrology IX* (Vol. 6742,

p. 67420N). International Society for Optics and Photonics. https://doi.org/https://doi.org/10.1117/12.769056

Saran, S., Sterk, G., & Kumar, S. (2009). Optimal land use/land cover classification using remote sensing imagery for hydrological modeling in a Himalayan watershed. *Journal of Applied Remote Sensing, 3*(1), 033551.

Saran, S., Sterk, G., Nair, R., & Chatterjee, R. S. (2014). Estimation of near surface soil moisture in a sloping terrain of a Himalayan watershed using ENVISAT ASAR multi-incidence angle alternate polarisation data. *Hydrological Processes, 28*(3), 895–904. https://doi.org/10.1002/hyp.9632.

Saran, S., Sterk, G., Peters, P., & Dadhwal, V. K. (2010). Evaluation of digital elevation models for delineation of hydrological response units in a himalayan watershed. *Geocarto International, 25*(2), 105–122. https://doi.org/10.1080/10106040903051967.

Semmens, D. J., Goodrich, D. C., Unkrich, C. L., Smith, R. E., Woolhiser, D. A., & Miller, S. N. (2007). KINEROS2 and the AGWA modelling framework. *Hydrological Modelling in Arid and Semi-Arid Areas,* . https://doi.org/10.1017/CBO9780511535734.006.

Siakeu, J., & Oguchi, T. (2000). Soil erosion analysis and modelling: A review. *Chikei*.

Sidman, G., Guertin, D. P., Goodrich, D. C., Unkrich, C. L., & Burns, I. S. (2016). Risk assessment of post-wildfire hydrological response in semiarid basins: the effects of varying rainfall representations in the KINEROS2/AGWA model. *International Journal of Wildland Fire, 25*(3), 268–278. https://doi.org/10.1071/WF14071.

Smith, R. E., Goodrich, D. C., & Unkrich, C. L. (1999). Simulation of selected events on the Catsop catchment by KINEROS2. A report for the GCTE conference on catchment scale erosion models. *CATENA, 37*(3–4), 457–475. https://doi.org/10.1016/S0341-8162(99)00033-8.

Smith, R. E., Goodrich, D. C., Woolhiser, D. A., & Unkrich, C. L. (1995). Kineros: A kinematic runoff and erosion model. In *Computer models of watershed hydrology*.

Smith, R. E., & Parlange, J.-Y. (1978). A parameter-efficient hydrologic infiltration model. *Water Resources Research, 14*(3), 533–538. https://doi.org/10.1029/WR014i003p00533.

Smith, R. E., & Quinton, J. N. (2000). Dynamics and scale in simulating erosion by water. In *Soil erosion* (pp. 283–294). Springer, Berlin, Heidelberg.

Srivastava, H. S., Patel, P., Manchanda, M. L., & Adiga, S. (2003). Use of multiincidence angle RADARSAT-1 SAR data to incorporate the effect of surface roughness in soil moisture estimation. *IEEE Transactions on Geoscience and Remote Sensing, 41*(7), 1638–1640. https://doi.org/10.1109/TGRS.2003.813356.

Star, J. L., Estes, J. E., McGwire, K. C., Arvidson, R. E., & Rycroft, M. J. (Eds.). (1997). *Integration of geographic information systems and remote sensing,* (Vol. 5). Cambridge: Cambridge University Press.

Tiwari, P. C. (2000). Land-use changes in Himalaya and their impact on the plains ecosystem: Need for sustainable land use. *Land Use Policy, 17*(2), 101–111. https://doi.org/10.1016/S0264-8377(00)00002-8.

Ulaby, F. T., Moore, R. K., & Fung, A. K. (1986). Microwave remote sensing: active and passive. Volume III: from theory to applications. *Microwave remote sensing: Active and passive. Volume III: From theory to applications.*

van Oevelen, P. J., & Hoekman, D. H. (1994). Estimation of areal soil water content during HAPEX-Sahel and EFEDA-Spain. In *International geoscience and remote sensing symposium (IGARSS),* (Vol. 3, pp. 1591-vol). IEEE. https://doi.org/https://doi.org/10.1109/igarss.1994.399507

Vrieling, A. (2006). Satellite remote sensing for water erosion assessment: A review. *CATENA, 65*(1), 2–18. https://doi.org/10.1016/j.catena.2005.10.005.

Wigmosta, M. S., Vail, L. W., & Lettenmaier, D. P. (1994). A distributed hydrology-vegetation model for complex terrain. *Water Resources Research, 30*(6), 1665–1679. https://doi.org/10.1029/94WR00436.

Wolock, D. M., & Price, C. V. (1994). Effects of digital elevation model map scale and data resolution on a topography-based watershed model. *Water Resources Research, 30*(11), 3041–3052. https://doi.org/10.1029/94WR01971.

Woolhiser, D. A., Hanson, C. L., & Kuhlman, A. R. (1970). Overland flow on rangeland watersheds. *Journal of Hydrology (New Zealand),* 336–356.

Woolhiser, D. A., Smith, R.-E., & Goodrich, D.-C. (1990). *KINEROS, a kinematic Runoff and Erosion Model: Documentation and User Manual*. Department of Agriculture, Agricultural Research Service: U.S.

Yatheendradas, S., Wagener, T., Gupta, H., Unkrich, C., Goodrich, D., Schaffner, M., & Stewart, A. (2008). Understanding uncertainty in distributed flash flood forecasting for semiarid regions. *Water Resources Research*. https://doi.org/10.1029/2007WR005940.

Ziegler, A. D., Giambelluca, T. W., & Sutherland, R. A. (2001). Erosion prediction on unpaved mountain roads in northern Thailand: validation of dynamic erodibility modelling using KINEROS2. *Hydrological Processes, 15*(3), 337–358.